

Quantification of the Plan Aperture Modulation of Radiotherapy Treatment Plans

Victor Hernandez

Department of Medical Physics, Hospital Sant Joan de Reus, IISPV, Tarragona, Spain
Universitat Rovira i Virgili (URV), Tarragona, Spain

Iñigo Lara-Aristimuño

Department of Medical Physics, Hospital Sant Joan de Reus, IISPV, Tarragona, Spain
Universitat Rovira i Virgili (URV), Tarragona, Spain

Ruben Abella

Department of Medical Physics, Hospital Sant Joan de Reus, IISPV, Tarragona, Spain

Jordi Saez

Department of Radiation Oncology, Hospital Clínic de Barcelona, Barcelona, Spain

Corresponding Author: Victor Hernandez, v hernandezmasgrau@gmail.com

Conflict of Interest: None

Funding Statement: This research was funded by the Spanish Society of Medical Physics (SEFM) through research Grant PI-SEFM-2022.

Data Sharing: Detailed research data will be shared upon reasonable request to the corresponding author.

Abstract

Purpose: This study introduces a novel metric, Plan Aperture Modulation (PAM), developed to quantify the modulation of radiotherapy treatment plans. PAM aims to provide a clear geometric interpretation, addressing the limitations of previous complexity metrics and facilitating its integration into treatment planning systems (TPSs) and clinical workflows.

Methods and Materials: The PAM metric was defined as the average fraction of the target area located outside the beam aperture, weighted over all control points in a treatment plan. The metric was evaluated in Volumetric Modulated Arc Therapy plans for two anatomical sites: prostate with lymph nodes and lung stereotactic body radiation therapy. Plans with varying complexities were generated using the Eclipse TPS, and PAM was compared to established metrics, including Plan Modulation (PM), Modulation Complexity Score (MCS), and monitor units per Gray (MU/Gy). The relationship between PAM and the Modulation Factor (MF), which quantifies the increase in MUs due to plan modulation, was also investigated.

Results: PAM provided a more intuitive and geometrically clear assessment of plan modulation compared to the other metrics, and was validated across different delivery systems, such as C-arm linacs and Halcyon systems. The metric outperformed the previous metrics, indicated a zero modulation for Dynamic Conformal Arc plans, and was independent of confounding variables, such as treatment technique, beam energy, delivery system, and patient anatomy. Derived equations enabled the calculation of MF based on PAM, allowing for a robust quantification of plan modulation.

Conclusions: PAM is a robust and intuitive metric for quantifying modulation in radiotherapy plans. It overcomes the limitations of previous metrics and can be readily implemented in TPSs to control plan modulation during optimization and for reporting. PAM is a promising tool for improving treatment planning workflows and for comparing and benchmarking radiotherapy plans in multi-institutional studies, clinical trials, and audits.

Introduction

Intensity-modulated radiotherapy (IMRT) is currently the standard treatment technique in radiotherapy, primarily due to its ability to produce highly conformal dose distributions and reduce the radiation doses delivered to organs at risk¹. The key principle of IMRT is to optimize the delivered fluence by modulating beam apertures either through static beam positions or dynamic arc delivery². This latter method forms the basis of volumetric modulated arc therapy (VMAT), where the beam aperture is modulated with a dynamic multileaf collimator (MLC), and treatment is delivered while the gantry rotates with variable dose rates and gantry speeds^{3,4}.

It is well established that IMRT techniques increase treatment complexity, which can introduce larger uncertainties in both the calculated and delivered doses, potentially compromising clinical treatment accuracy^{5,6}. As a result, dosimetric verifications are warranted to ensure the accuracy and reliability of clinical IMRT plans^{7,8}. The American Association of Physicists in Medicine (AAPM) emphasizes the importance of quantifying plan modulation⁹ and recommends checking the degree of plan modulation during the evaluation of IMRT patient-specific quality assurance (PSQA) results⁸. The Medical Physics Practice Guidelines for commissioning and quality assurance (QA) of treatment planning dose calculations further recommend clearly documenting the modulation amount and range of the treatment plans evaluated¹⁰. The TG-218 report even suggests adapting tolerance limits according to plan complexity and explicitly recommends replanning in cases of excessive modulation to prevent failures in treatment verifications⁸.

Despite these recommendations, there is still no clear consensus on how to quantify plan modulation^{11,12,13}. Traditionally, the number of monitor units (MUs) or the ratio of MUs to the prescribed fraction dose (MU/Gy) has been used as an indirect indicator of modulation, as highly modulated plans generally involve smaller apertures, leading to higher numbers of MUs¹⁴. However, the number of MUs is affected by other variables, such as beam delivery characteristics and patient anatomy. To address these confounding factors, quantitative metrics focusing on various aspects of plan complexity have been proposed^{5,6}. Some of these metrics specifically address plan modulation, such as the plan modulation (PM) metric by Du et al.¹⁵ and the modulation complexity score (MCS) introduced by McNiven et al¹⁶. While these methods provide valuable insights into modulation, they fail to address all influencing factors, motivating the need for a more comprehensive metric.

The purpose of this study is to introduce a novel metric, the Plan Aperture Modulation (PAM), designed to provide a more comprehensive quantification of treatment plan modulation. The aim of the metric is to offer a clear interpretation and to overcome the limitations of existing metrics, making it suitable for implementation in TPSs. This study defines the PAM metric, compares it with existing metrics, and provides recommendations for its clinical implementation.

Methods and Materials

Metrics to quantify plan modulation

The ratio of MU to the prescribed fraction dose (MU/Gy) and the complexity metrics PM and MCS were evaluated as indicators of plan modulation. Beam Modulation (BM) was defined for step-and-shoot IMRT as the difference between the area of each segment within a beam and the total beam aperture area, which was computed as the union of all segment apertures in the beam¹⁵. The BM metric was computed by averaging these differences for all segments in a beam, weighted by the MUs for each segment. PM was defined as the weighted average of BM across all beams within the treatment plan, with MU as the weighting factor¹⁵.

MCS was also first applied to step-and-shoot IMRT, integrating information about both segment area and shape¹⁶. MCS combines two parameters: Leaf Sequence Variability (LSV), which describes segment shape variability, and Aperture Area Variability (AAV), which quantifies segment area variations relative to the total combined aperture. MCS decreases with increasing complexity and ranges from 1.0 (single rectangular open beam) to 0, as smaller and irregular segments are added. MCS, therefore, offers a composite metric that is closely related to the modulation of beam apertures. These metrics can be adapted to VMAT by considering the apertures at each control point¹⁷.

New metric: Plan Aperture Modulation (PAM)

We developed a new metric to characterize the modulation of beam apertures and compared it with the PM and MCS metrics. First, Aperture Modulation (AM) is defined at each control point as the ratio of the target projection area outside the beam aperture to the

total target projection area:

$$AM = \frac{A_{\text{blocked}}}{A_{\text{total}}} \quad , \quad (1)$$

where A_{total} is the total area of the target projection in the beam's eye view (BEV) and A_{blocked} is the area of the target projection outside the beam aperture, i.e., blocked by the MLC or jaws. Figure 1 illustrates an example of these concepts at a given control point.

The PAM metric is calculated by averaging the AM values across all control points, weighted by the number of MUs delivered at each control point j :

$$PAM = \frac{\sum_j AM_j * MU_j}{\sum_j MU_j} \quad . \quad (2)$$

PAM represents the weighted average fraction of the target projection outside the beam aperture across all control points within a treatment plan. This metric ranges from 0 (indicating no modulation, the entire target always included within the BEV) to 1 (target fully blocked), and offers a clear geometrical interpretation that aligns with the intuitive concept of aperture modulation. The same approach can be used to compute the modulation of individual IMRT beams, where the term 'Beam' Aperture Modulation (BAM) should be applied. BAM is calculated by summing the contributions from control points specific to an individual beam.

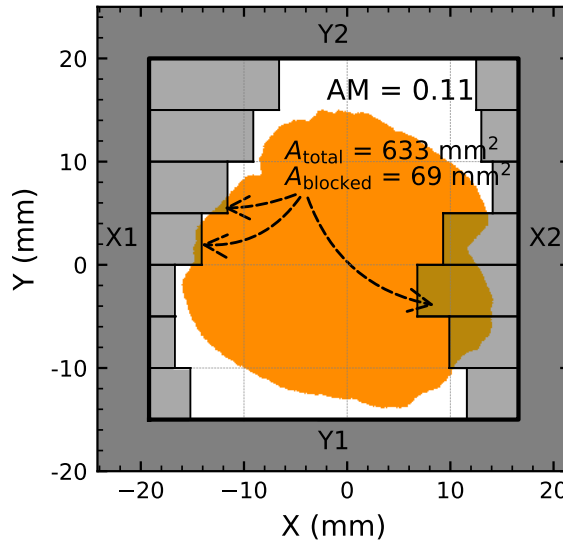


Figure 1: Sketch illustrating the beam aperture and the target projection in the beam's eye view. The total area of the target projection (A_{total}), the area of the target projection outside the beam aperture (A_{blocked}), and the corresponding AM value are given as an example.

The relationship between delivered dose, the number of MUs, and PAM can be estimated using approximations^{18,19,20}, and is analytically derived in Appendix A. This relationship is given by:

$$D = k_{\text{eff}} * MU * [1 - PAM(1 - T)] , \quad (3)$$

where D is the delivered dose to the structure, T is the average transmission, and k_{eff} is a case-specific factor depending on the beam geometry and patient anatomy.

Cases and treatment plans evaluated

To demonstrate the behavior of the PAM metric, we evaluated two anatomical sites: prostate with lymph nodes and lung stereotactic body radiation therapy (SBRT). The prostate cases included two target volumes: a high-dose prostate volume (70 Gy) and lymph nodes receiving between 50.4 Gy or 54 Gy. The lung SBRT cases involved a single target volume prescribed to 60 Gy in either 3 or 5 fractions.

For each site, five cases were selected, and multiple VMAT plans with varying plan complexities were generated using the Eclipse TPS (v16.1, Varian Medical Systems) for a Varian TrueBeam equipped with a Millennium 120 MLC and using jaw tracking. Prostate plans used 6 MV with a flattening filter, while lung SBRT plans used 6 MV flattening filter-free (FFF). Prostate plans involved two full arcs, and lung SBRT plans used 3–4 partial arcs. For comparison purposes, five additional head-and-neck plans were also produced, and a few prostate plans were reoptimized for the TrueBeam using 10 MV and for a Halcyon system using 6 MV FFF.

To produce plans with different levels of complexity, plans were first optimized without any specific control of plan complexity: the Aperture Shape Controller (ASC)²¹ was first set to ‘Off’ during optimization, with no restrictions on MU. Subsequently, the ASC was set to ‘Moderate’ and the plan was reoptimized preserving the same optimization objectives. Finally, the plans were again reoptimized keeping the ASC to ‘Moderate’ and reducing the number of MUs. For the lung SBRT cases, dynamic conformal arc (DCA) plans were also generated, where MLCs continuously conformed to the target without intensity modulation²².

Computations and comparisons of complexity metrics

PM and MCS were computed using PlanAnalyzer, a MATLAB-based tool that processes DICOM RTPlan data exported from the TPS²³. A Python script (version 3.11) was developed to calculate the PAM metric from DICOM objects exported from the TPS, ensuring compatibility with any TPS. The DICOM RT-structure set contours were first rasterized into a 3D array and meshed using the marching cubes algorithm (*scikit-image* library). Next, the 3D mesh was projected into the BEV using the open-3d library, with beam aperture projections obtained from MLC and jaw positions. Finally, the total area (A_{total}) and blocked area (A_{blocked}) of the projected structure were obtained at each control point from the number of structure pixels inside and outside the beam aperture and the PAM metric was obtained using Equations 1 and 2.

To validate the previous code and compute PAM directly within the Eclipse TPS, a C# program was developed using the Eclipse Scripting Application Programming Interface (ESAPI). The 3D mesh, directly available from the TPS through ESAPI, and the *System.Windows.Media.Media3D* library were used to project the structure in the BEV with a resolution of 0.625 mm. This resolution, coarser than that employed in the Python script, was selected to reduce computation times within the TPS. Finally, the beam aperture in the BEV was generated from the MLC and jaw positions, using the same resolution, and AM and PAM values were calculated. The developed codes are available upon request to the authors.

Results

Plan Modulation

The results for the PAM metric are presented in Figure 2, where the high-dose prostate was used as the target volume for the analysis. PAM values increased with plan complexity, with the lowest values occurring when both the ASC and the MU restrictions were applied (indicating the least complexity). For the SBRT lung cases, PAM values decreased to zero for the DCA plans, which involve no modulation.

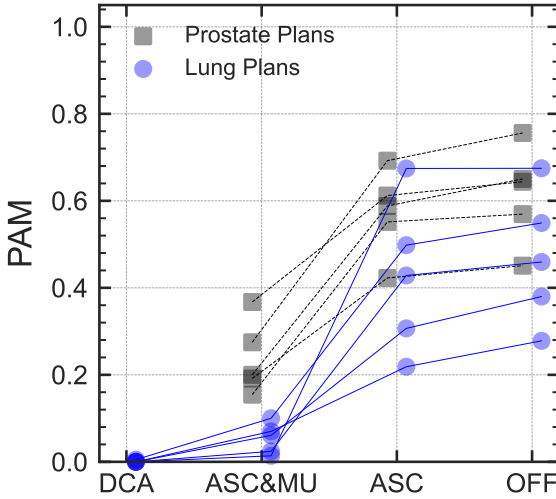


Figure 2: PAM values for prostate (focusing on the high-dose prostate volume) and lung SBRT plans. Symbols represent plans with different degrees of plan complexity and lines connect plans corresponding to the same clinical cases. X-axis labels indicate the control of plan complexity during optimization. OFF: No control of plan complexity; ASC: Aperture Shape Controller set to moderate; ASC&MU: Aperture Shape Controller set to moderate and restriction on the number of Monitor Units; DCA: Dynamic Conformal Arc technique.

Results from other metrics are shown in Figure 3. The MU/Gy values exhibited trends similar to PAM but did not converge to a common value for DCA plans. PM showed a similar trend, with values increasing alongside plan complexity. However, for DCA plans, PM values ranged from 0.15 to 0.30 instead of decreasing to zero. As expected, MCS values generally decreased with increasing complexity but, surprisingly, MCS values for DCA plans were smaller than those for ASC&MU, indicating higher complexity despite the lack of aperture modulation.

A direct comparison of these metrics with PAM is shown in Figure 4. In general, clear trends were obtained between PAM and the other metrics, but large variations were found between different anatomical sites and also across plans from the same site.

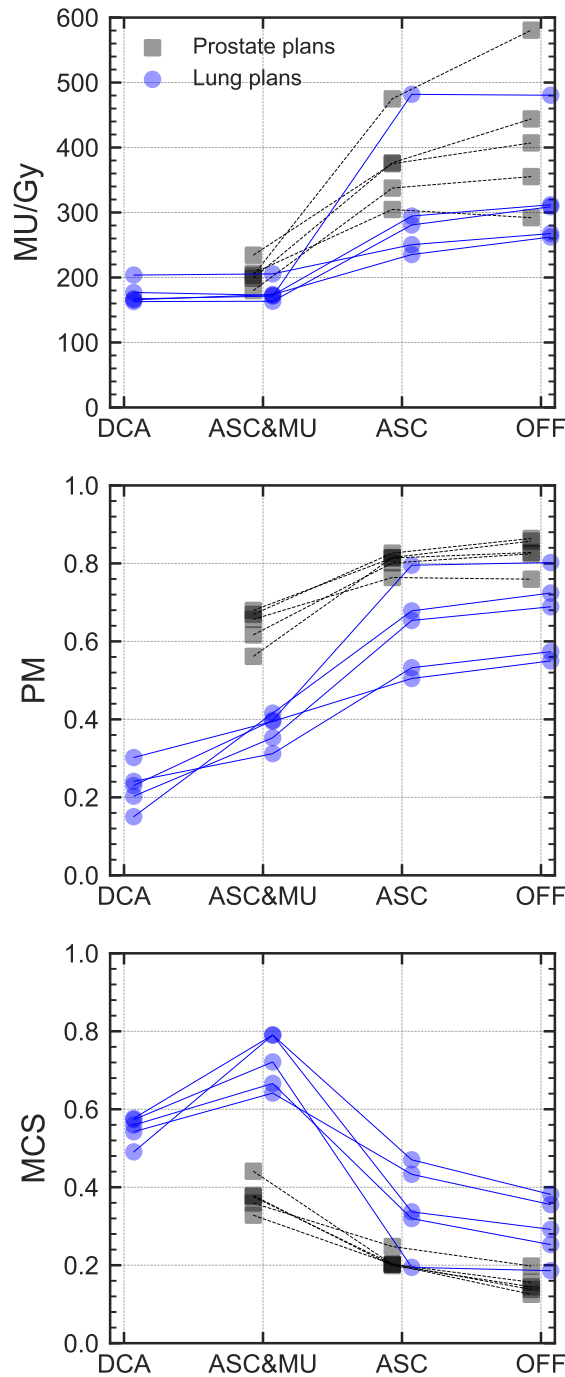


Figure 3: Plan complexity values for prostate and lung SBRT plans for three different metrics: ratio of Monitor Units to prescribed dose (MU/Gy, upper row), Plan Modulation (PM, middle row), and Modulation Complexity Score (MCS, lower row). Symbols represent plans with different degrees of complexity and lines connect plans corresponding to the same clinical cases. X-axis labels indicate the control of plan complexity during optimization. OFF: No control of plan complexity; ASC: Aperture Shape Controller set to moderate; ASC&MU: Aperture Shape Controller set to moderate and restriction on the number of Monitor Units; DCA: Dynamic Conformal Arc technique.

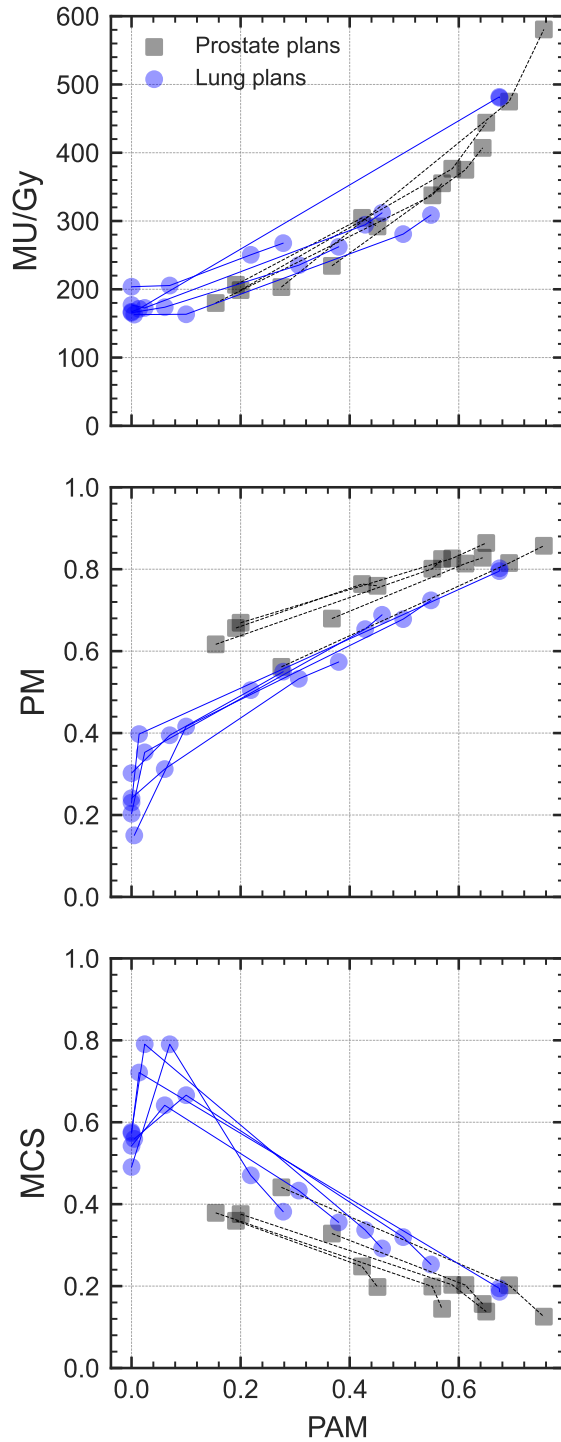


Figure 4: Relationship between PAM values and number of Monitor Units per Gray (MU/Gy, upper row), Plan Modulation (PM, middle row), and Modulation Complexity Score (MCS, lower row). Symbols represent plans with different degrees of complexity, distinguishing between lung SBRT and prostate plans. Lines connect plans from the same clinical cases.

Relationship between Monitor Units and PAM: Modulation Factor

The relationship between MU/Gy and PAM was further explored using Equation 3. For two treatment plans (denoted as ‘1’ and ‘2’) from the same clinical case, the equation shows that:

$$MU_1 * [1 - PAM_1(1 - T)] = MU_2 * [1 - PAM_2(1 - T)] , \quad (4)$$

where k_{eff} cancels out, as it is assumed to remain constant for plans that differ exclusively in their level of complexity control while preserving the same beam arrangement (such as the number of arcs and the arc span).

If the number of MUs and the PAM value are known for one plan, the MU-PAM relationship for another plan from the same case can be derived. The relationship between PAM and MU can be expressed as:

$$PAM_2 = \frac{MU_2 - MU_1[1 - PAM_1(1 - T)]}{MU_2(1 - T)} . \quad (5)$$

The reverse relationship, where MU is derived from PAM, is given by:

$$MU_2 = MU_1 * \frac{1 - PAM_1(1 - T)}{1 - PAM_2(1 - T)} . \quad (6)$$

Figure 5 shows the PAM and MU/Gy values for several plans from two different clinical cases, illustrating differences due to the treatment site, energy, and delivery system. However, discrepancies between computed and predicted values were minimal, validating the accuracy of the derived equations. This held true even when different techniques, such as VMAT and sliding windows, were used.

To address these differences, the Modulation Factor (MF) was defined as the ratio of the MU (or MU/Gy) of a given plan and its predicted value for PAM = 0:

$$MF = \frac{MU}{MU_{PAM=0}} . \quad (7)$$

Using Equation 6, this expression can be rewritten as:

$$MF = \frac{1}{1 - PAM * (1 - T)} . \quad (8)$$

The lower row in Figure 5 illustrates the relationship between MF and PAM, highlighting how MF removes the previous case-specific differences, including those due to treatment site,

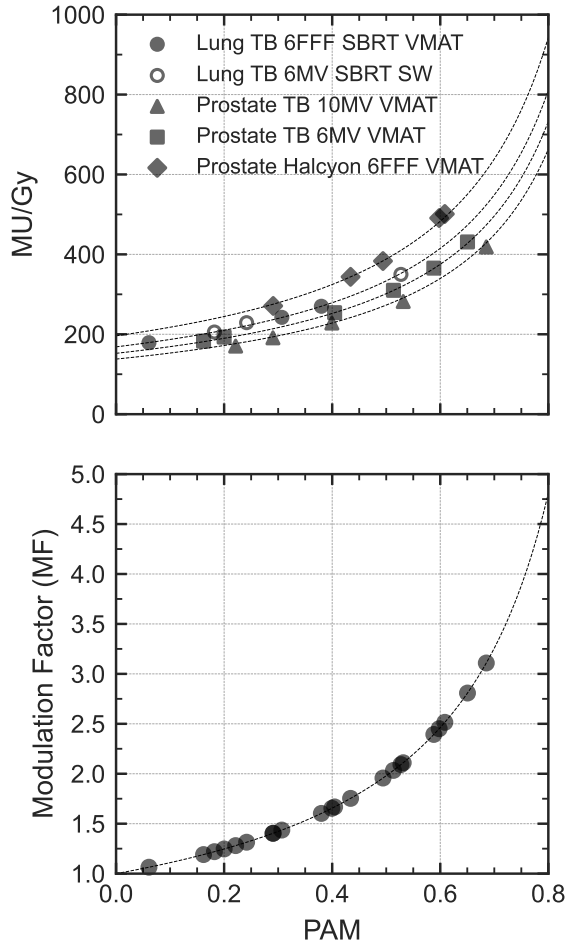


Figure 5: Upper row: Relationship between the number of Monitor Units (MU) and PAM values for two clinical cases and various plans using different energies and treatment techniques - Volumetric Arc Therapy (VMAT), Sliding Windows (SW), and Dynamic Arc Therapy (DCA). The lines show the relationship between MU and PAM given by Equation 5. Lower row: Modulation Factor for the same plans, with lines indicating the theoretical predicted values given by Equation 8.

energy, and delivery system. Moreover, the predictions from Equation 8 closely aligned with the calculated MF values, validating the derived relationship.

Plans with simultaneous integrated boost (SIB)

For IMRT plans with simultaneous integrated boost, where multiple target volumes are prescribed different dose levels^{24,25}, the PAM value depends on the structure selected for analysis. Figure 6 shows the relationship between prescribed dose and PAM for different

target structures, showing that structures receiving higher doses have lower PAM values, while those with lower doses exhibit larger PAM values due to the greater proportion of blocked apertures required to achieve a lower dose in that target.

The relationship between PAM values for different structures can be expressed analytically using Equation 3:

$$\frac{1 - PAM_2(1 - T)}{D_2/k_{\text{eff}}_2} = \frac{1 - PAM_1(1 - T)}{D_1/k_{\text{eff}}_1} , \quad (9)$$

where the number of MU cancels out because both sides of the equation correspond to the same plan. Using this relationship, the PAM value for structure ‘2’ can be estimated from the PAM value of structure ‘1’, the ratio of prescribed doses, and a correction factor C that depends on the specific geometry of each structure ($C = k_{\text{eff}}_1/k_{\text{eff}}_2$):

$$PAM_2 = \frac{1 - C * D_2/D_1 * [1 - PAM_1 * (1 - T)]}{1 - T} \quad (10)$$

This equation shows that PAM value for a given structure varies linearly with D , but the proportionality coefficient depends on both the transmission T and the geometry of each target volume (through the constant C). The additional head-and-neck plans in Figure 6 more clearly illustrate this relationship due to the three dose levels used. A deviation from linearity is observed across different structures due to variations in geometry, but PAM values consistently increased as relative doses decreased.

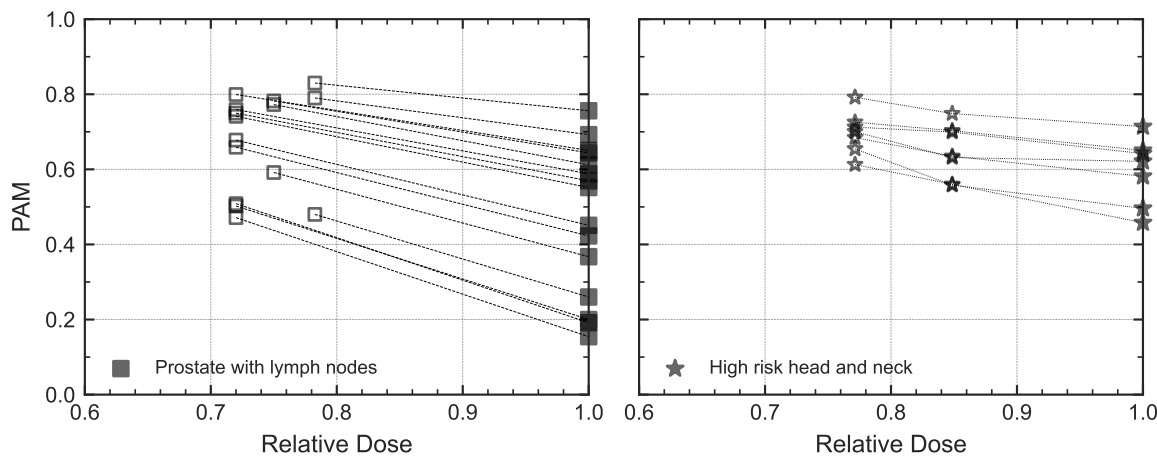


Figure 6: PAM values for prostate lymph nodes (left) and head-and-neck plans (right) as a function of their relative dose (with respect to the highest-dose target). Lines connect data points from the same treatment plans, corresponding to different target volumes.

Discussion

Plan complexity metrics were originally derived from fluence maps, measuring variations in photon fluence between adjacent pixels^{26,27}. However, fluence-based metrics present inherent limitations, as they do not account for the fact that beam segmentation can vary while producing identical total fluence maps¹⁵. Additionally, modern optimization algorithms are no longer fluence-based, focusing instead on the direct optimization of machine-specific parameters²⁸. Consequently, fluence-based metrics have been progressively replaced by metrics that incorporate specific plan parameters, such as MLC positions^{5,6}.

However, these newer metrics also have inherent limitations. For instance, PM and MCS were developed for static-gantry IMRT, with the union of segments of a given beam serving as a surrogate for the total projection of the target structure in the BEV for that gantry angle^{15,16}. In VMAT plans, however, the continuous change in target volume projection with gantry rotation reduces the interpretation of these metrics as ‘absolute’ values, complicating their applicability²⁹. Unlike MCS and PM, PAM is inherently independent of beam energy, output calibration, and patient anatomy, providing a more universal metric for plan modulation.

The PAM’s ability to derive the MF is particularly useful, as MF is defined as the factor by which the number of MUs increases due to aperture modulation and also provides a clear interpretation. Figure 5 shows the relationship between MF and PAM, with MF increasing linearly for PAM values up to 0.4 and rising more rapidly at higher PAM values. Notably, MF can also be computed for individual beams by replacing PAM with BAM. A disadvantage of MF is that it depends slightly on the delivery system through the average transmission T , but its impact is minimal, particularly for clinical plans with $PAM < 0.75$. In this study, $T = 0.01$ was used, which is a value slightly lower than the average MLC transmission, to account for both MLC transmission and jaw tracking.

In summary, PAM offers several key advantages:

- It can quantify the modulation of both entire treatment plans and individual IMRT beams.
- It offers a clear geometric interpretation that aligns with the intuitive concept of the modulation of beam apertures.
- It is independent of beam characteristics and patient anatomy.

- It can be applied to any delivery system and treatment technique, regardless of collimating devices.
- It facilitates the computation of MF.

The primary applications of PAM are expected to be in controlling plan modulation during the optimization processes and in reporting modulation degrees. Reducing plan modulation is essential to decrease uncertainties in IMRT/VMAT plans, thereby improving the accuracy and robustness of TPS calculations and treatment deliveries^{30,31,32}. Most TPSs currently control plan modulation through the number of MUs, but PAM and MF offer distinct advantages that clearly outperform MUs in this role.

We advocate for the integration of PAM and MF metrics in TPS platforms. Until such tools are implemented, external tools can be used to incorporate these metrics into treatment planning workflows. For example, once PAM is calculated, the corresponding number of MUs needed to achieve a lower PAM value can be determined and applied as a constraint within the TPS optimizer. A script has been developed to calculate PAM within the TPS, eliminating the need to export plans or structure sets.

Modern radiotherapy techniques, such as treatments involving multiple target volumes and simultaneous integrated boosts, present additional challenges in quantifying plan modulation. In these scenarios, PAM values for high-dose targets are lower than for low-dose targets, which have a greater proportion of blocked apertures. As a result, the highest dose target typically determines the minimum modulation required for clinically acceptable dose distributions, making it more effective to control plan modulation by focusing on these high-dose volumes.

Quantifying the degree of plan modulation is essential for evaluating and comparing treatment plans, assessing overall plan quality, estimating uncertainties, and optimizing PSQA workflows^{5,6,12}. We demonstrated that PAM is applicable to various delivery systems, including C-arm linacs and Halcyon systems with double-stacked MLCs, and it is expected to perform well with other systems, such as CyberKnife and TomoTherapy.

Multicentric comparisons represent another critical application. While reporting plan modulation and complexity is strongly recommended³³, these recommendations are often not fulfilled, likely due to the absence of suitable metrics. PAM offers a promising solution for comparing and benchmarking treatment plans across multiple institutions, particularly

in clinical trials and audits.

Despite its advantages, PAM is more complex to compute than metrics based solely on plan parameters due to the need for BEV projections, which increases computational requirements. However, our comparisons between the Python and C# codes showed good agreement, with most differences < 0.01 , and reasonable computation times. The Python code required 4 to 30 seconds, depending on target size and the number of control points, while the TPS script was faster (1-5 seconds), due to the larger resolution used and the availability of the 3D mesh through ESAPI. Modern TPSs platforms typically include built-in tools for BEV projections, which can significantly accelerate computations and facilitate efficient implementation. Moreover, TPS optimizers can typically estimate the number of MUs during the optimization process, and the relationship between PAM and MUs is well determined. Therefore, PAM could be used to control plan modulation during optimization by estimating it through the number of MUs, without the need for recalculation at every iteration.

One limitation of this study is that it did not address other aspects of plan complexity, such as aperture irregularity¹⁵, speed and distance traveled by the leaves¹⁷, or variations in dose rate and gantry speed³⁴. While the modulation of beam apertures has been regarded as the primary component of plan complexity¹², other characteristics may also be relevant. To fully characterize the complexity of IMRT/VMAT plans, it will be important to complement the quantification of aperture modulation with metrics that capture additional plan attributes²³.

Another limitation is that we did not investigate the minimum degree of plan modulation necessary for achieving clinically acceptable plans, the relationship with PSQA results, or other potential applications of the proposed metric. These investigations require careful analysis and will be the focus of future work.

Conclusions

The Plan Aperture Modulation (PAM) metric was introduced to quantitatively assess the modulation in radiotherapy treatment plans. PAM offers a robust and intuitive measure of plan modulation, addressing limitations of previous metrics and allowing for the calculation of the Modulation Factor MF, which quantifies the increase in MUs due to aperture modulation. PAM can be readily integrated into TPSs to control plan modulation during optimization processes and for reporting. It offers a promising tool for improving radiotherapy treatment planning workflows, facilitating robust comparison and benchmarking of plans in multi-institutional studies, clinical trials, and audits.

Appendix: Analytical Relationship Between PAM, Delivered Dose, and Monitor Units

The relationship between PAM, delivered dose, and MUs can be derived analytically following a strategy based on the estimation of the total fluence^{18,19,20}. The total fluence delivered to a structure by a given beam aperture at a control point j is directly proportional to the number of MUs and the irradiated area receiving a given transmission:

$$\varphi_j = \alpha_j * MU_j * [A_{\text{open},j} * 1 + A_{\text{blocked},j} * T] , \quad (\text{A1})$$

where A_{open} is the area of the projected structure within the beam aperture (with transmission = 1), A_{blocked} is the area of the projected structure outside the beam aperture, T is the average transmission of the beam collimating device (e.g., the MLC), and α is the proportionality constant. Since $A_{\text{total}} = A_{\text{open}} + A_{\text{blocked}}$ and using Equation 1, Equation A1 can be rewritten as:

$$\varphi_j = \alpha_j * MU_j * [A_{\text{total},j} - A_{\text{blocked},j} (1 - T)] = \alpha_j * MU_j * A_{\text{total},j} * [1 - AM_j * (1 - T)] . \quad (\text{A2})$$

The delivered dose D is directly proportional to the fluence density, which can be approximated as the ratio of the total delivered fluence to the total area of the projected

structure:

$$D_j = \beta_j \frac{\varphi_j}{A_{\text{total},j}} = k_j * MU_j * [1 - AM_j * (1 - T)] \quad , \quad (\text{A3})$$

where the constants α_j and β_j are combined into $k_j = \alpha_j * \beta_j$.

The plan dose D is then obtained by summing the contributions from all control points:

$$D = \sum_j D_j = \sum_j k_j * MU_j * [1 - AM_j * (1 - T)] \quad . \quad (\text{A4})$$

The distribution of k_j factors depends on the patient's anatomy and beam setup but, for a given plan, an effective factor k_{eff} can be used, resulting in:

$$D = k_{\text{eff}} \sum_j MU_j * [1 - AM_j * (1 - T)] \quad . \quad (\text{A5})$$

Rearranging terms, we can express D as:

$$D = k_{\text{eff}} \left[MU - \sum_j MU_j * AM_j * (1 - T) \right] = k_{\text{eff}} MU \left[1 - \frac{\sum_j MU_j * AM_j}{MU} (1 - T) \right] \quad . \quad (\text{A6})$$

From Equation 2 and Equation A6, it follows that:

$$D = k_{\text{eff}} * MU * [1 - PAM(1 - T)] \quad . \quad (\text{A7})$$

Thus, Equation A7 provides an approximate analytical relationship between dose, MUs, PAM, and average transmission T .

References

¹ Cedric XY, Li XA, Ma L, et al. Clinical implementation of intensity-modulated arc therapy. *Int J Radiat Oncol Biol Phys* 2002;53:453–463.

² Bortfeld T. IMRT: a review and preview. *Phys Med Biol* 2006;51:R363–R379.

³ Otto K. Volumetric modulated arc therapy: IMRT in a single gantry arc. *Med Phys* 2008;35:310–317.

⁴ Matuszak MM, Yan D, Grills I, Martinez A. Clinical applications of volumetric modulated arc therapy. *Int J Radiat Oncol Biol Phys* 2010;77:608–616.

⁵ Chiavassa S, Bessieres I, Edouard M, Mathot M, Moignier A. Complexity metrics for IMRT and VMAT plans: a review of current literature and applications. *Br J Radiol* 2019;92:20190270.

⁶ Antoine M, Ralite F, Soustiel C, et al. Use of metrics to quantify IMRT and VMAT treatment plan complexity: A systematic review and perspectives. *Phys Med* 2019;64:98–108.

⁷ Low DA, Moran JM, Dempsey JF, Dong L, Oldham M. Dosimetry tools and techniques for IMRT. *Med Phys* 2011;38:1313–1338.

⁸ Miften M, Olch A, Mihailidis D, et al. Tolerance limits and methodologies for IMRT measurement-based verification QA: Recommendations of AAPM Task Group No. 218. *Med Phys* 2018;45:e53–e83.

⁹ Ezzell GA, Burmeister JW, Dogan N, et al. IMRT commissioning: Multiple institution planning and dosimetry comparisons, a report from AAPM Task Group 119. *Med Phys* 2009;36:5359–5373.

¹⁰ Geurts MW, Jacqmin DJ, Jones LE, et al. AAPM MEDICAL PHYSICS PRACTICE GUIDELINE 5. b: Commissioning and QA of treatment planning dose calculations—Megavoltage photon and electron beams. *J Appl Clin Med Phys* 2022;23:e13641.

¹¹ Kamperis E, Kodona C, Hatzioannou K, Giannouzakos V. Complexity in Radiation Therapy: It's Complicated. *Int J Radiat Oncol Biol Phys* 2020;106:182–184.

¹² Hernandez V, Hansen CR, Widesott L, et al. What is plan quality in radiotherapy? The importance of evaluating dose metrics, complexity, and robustness of treatment plans. *Radiother Oncol* 2020.

¹³ Kaplan LP, Placidi L, Bäck A, et al. Plan quality assessment in clinical practice: Results of the 2020 ESTRO survey on plan complexity and robustness. *Radiother Oncol* 2022;173:254–261.

¹⁴ Craft D, Süss P, Bortfeld T. The tradeoff between treatment plan quality and required number of monitor units in intensity-modulated radiotherapy. *Int J Radiat Oncol Biol Phys* 2007;67:1596–1605.

¹⁵ Du W, Cho SH, Zhang X, Hoffman KE, Kudchadker RJ. Quantification of beam complexity in intensity-modulated radiation therapy treatment plans. *Med Phys* 2014;41:021716.

¹⁶ McNiven AL, Sharpe MB, Purdie TG. A new metric for assessing IMRT modulation complexity and plan deliverability. *Med Phys* 2010;37:505–515.

¹⁷ Masi L, Doro R, Favuzza V, Cipressi S, Livi L. Impact of plan parameters on the dosimetric accuracy of volumetric modulated arc therapy. *Med Phys* 2013;40:071718.

¹⁸ Arnfield MR, Siebers JV, Kim JO, Wu Q, Keall PJ, Mohan R. A method for determining multileaf collimator transmission and scatter for dynamic intensity modulated radiotherapy. *Med Phys* 2000;27:2231–2241.

¹⁹ Cedric XY. Design considerations for the sides of multileaf collimator leaves. *Phys Med Biol* 1998;43:1335.

²⁰ Saez J, Hernandez V, Goossens J, De Kerf G, Verellen D. A novel procedure for determining the optimal MLC configuration parameters in treatment planning systems based on measurements with a Farmer chamber. *Phys Med Biol* 2020;65:155006.

²¹ Scaggion A, Fusella M, Agnello G, et al. Limiting treatment plan complexity by applying a novel commercial tool. *J Appl Clin Med Phys* 2020;21:27–34.

²² Bokrantz R, Wedenberg M, Sandwall P. Dynamic conformal arcs for lung stereotactic body radiation therapy: a comparison with volumetric-modulated arc therapy. *J Appl Clin Med Phys* 2020;21:103–109.

²³ Hernandez V, Saez J, Pasler M, Jurado-Bruggeman D, Jornet N. Comparison of complexity metrics for multi-institutional evaluations of treatment plans in radiotherapy. *Phys Imaging Radiat Oncol* 2018;5:37-43.

²⁴ Popple RA, Prellup PB, Spencer SA, et al. Simultaneous optimization of sequential IMRT plans. *Med Phys* 2005;32:3257-3266.

²⁵ Jolly D, Alahakone D, Meyer J. A RapidArc planning strategy for prostate with simultaneous integrated boost. *J Appl Clin Med Phys* 2011;12:35-49.

²⁶ Webb S. Use of a quantitative index of beam modulation to characterize dose conformality: illustration by a comparison of full beamlet IMRT, few-segment IMRT (fsIMRT) and conformal unmodulated radiotherapy. *Phys Med Biol* 2003;48:2051.

²⁷ Giorgia N, Antonella F, Eugenio V, Alessandro C, Filippo A, Luca C. What is an acceptably smoothed fluence? Dosimetric and delivery considerations for dynamic sliding window IMRT. *Radiat Oncol* 2007;2:1-13.

²⁸ Unkelbach J, Bortfeld T, Craft D, et al. Optimization approaches to volumetric modulated arc therapy planning. *Med Phys* 2015;42:1367-1377.

²⁹ Masi L, Hernandez V, Saez J, Doro R, Livi L. Robotic MLC-based plans: A study of plan complexity. *Med Phys* 2021;48:942-952.

³⁰ Younge KC, Roberts D, Janes LA, Anderson C, Moran JM, Matuszak MM. Predicting deliverability of volumetric-modulated arc therapy (VMAT) plans using aperture complexity analysis. *J Appl Clin Med Phys* 2016;17:124-131.

³¹ May L, Hardcastle N, Hernandez V, Saez J, Rosenfeld A, Poder J. Multi-institutional investigation into the robustness of intra-cranial multi-target stereotactic radiosurgery plans to delivery errors. *Med Phys* 2024;51:910-921.

³² May L, Barnes M, Hardcastle N, et al. Multi-institutional investigation into the robustness of intra-cranial multi-target stereotactic radiosurgery plans to patient setup errors. *Phys Med* 2024;124:103423.

³³ Hansen CR, Crijns W, Hussein M, et al. Radiotherapy Treatment plannINg study Guidelines (RATING): A framework for setting up and reporting on scientific treatment planning studies. *Radiother Oncol* 2020;153:67-78.

³⁴ Park JM, Park SY, Kim H, Kim JH, Carlson J, Ye SJ. Modulation indices for volumetric modulated arc therapy. *Phys Med Biol* 2014;59:7315-7340.